Electronic, magnetic, and transport properties and magnetic phase transition in quaternary (Cu,Ni)MnSb Heusler alloys

J. Kudrnovský
Institute of Physics, Academy of Sciences of the Czech Republic, CZ-182 21 Praha 8, Czech Republic and Institut für Mikrostrukturphysik, Max-Planck Institut, Weinberg 2, D-06120 Halle, Germany

V. Drchal
Institute of Physics, Academy of Sciences of the Czech Republic, CZ-182 21 Praha 8, Czech Republic

I. Turek
Department of Condensed Matter Physics, Faculty of Mathematics and Physics, Charles University, Ke Karlovu 5, CZ-12116 Prague 2, Czech Republic

P. Weinberger
Center for Computational Nanoscience, Seilerstätte 10/22, A-1010 Vienna, Austria
(Received 2 June 2008; revised manuscript received 14 July 2008; published 25 August 2008)

The electronic properties, finite-temperature magnetism, and transport properties of semi-Heusler quaternary alloys (Cu,Ni)MnSb are studied theoretically by means of *ab initio* calculations as a function of the alloy composition. As documented by experiment, the transition from the ferromagnetic state (NiMnSb) to the antiferromagnetic state (CuMnSb) gives rise to an abrupt change in the magnetic moments and resistivities at about $x_{\mathrm{Cu}} \approx 0.7$, while the Curie temperature exhibits a smooth behavior with the Cu content. We explain this peculiar behavior with the onset of disorder in orientations of the Mn spins at $x_{\mathrm{Cu}} \approx 0.7$. A simple account of magnetic disorder based on the so-called uncompensated disordered local-moment picture provides a good quantitative understanding of available experimental data. An origin of the observed magnetic phase transition is also discussed.

DOI: 10.1103/PhysRevB.78.054441 PACS number(s): 75.10.Hk, 71.22.+i, 72.25.Ba, 75.30.Et

I. INTRODUCTION

Ferromagnetic (FM) Heusler and semi-Heusler alloys are materials with interesting physical properties. Because of their halfmetallic character, structural similarity with semiconductors, and Curie temperatures above the room temperature, they represent materials with potential applications in spintronics. These properties motivated recent theoretical and experimental interests in these compounds such as, for example, the recent theoretical studies of Galanakis[1] and Sasioglu.[2] A summary of experimental and previous theoretical studies can be found in Ref. 3. The study of conventional ordered Heusler alloys is now rather a standard procedure; the situation for disordered Heusler alloys (quaternary alloys), however, differs. Recently the properties of disordered Heusler and semi-Heusler alloys were studied theoretically[4,5] by treating the effect of disorder properly within the framework of the coherent-potential approximation (CPA).

The system (Cu,Ni)MnSb is of particular interest as the end-point alloys NiMnSb and CuMnSb are FM and antiferromagnetic (AFM), respectively. It should be noted that while theoretical and experimental studies of NiMnSb are frequently found in the literature (see, e.g., Refs. 2–4), CuMnSb was studied rarely; the most complete theoretical study being that of Ref. 6. Very recently extensive experimental investigations of various properties of (Cu,Ni)MnSb quaternary alloys including magnetic, thermodynamic (Curie temperature), and transport properties were performed.[7,8] The main conclusion from these experimental studies is a dramatic change in the magnetization and the resistivity with a pronounced break at about 70% of Cu content, while for the Curie temperature a smooth concentration behavior was observed. Such a behavior can be qualitatively understood as the onset of disorder in spin orientations on the structurally perfect Mn sublattice induced by the chemical disorder on the (Cu,Ni) sublatice. Such a disorder will clearly reduce the spin magnetic moments and, at the same time, will increase the resistivity of the alloy. Because the large rigid moments on the Mn sites seem to be responsible for the thermodynamics of the system, it is reasonable to assume that exchange integrals will be only weakly influenced by magnetic disorder. In different words, one can assume that the estimated exchange interactions will only weakly depend on the reference magnetic state. This is in accord with a pair-exchange interaction Heisenberg model, for which one expects no dependence of the exchange integrals on the relative rotation angle between spin pairs. Since the alloy composition changes the carrier concentration (due to the different Cu and Ni valencies), the correspondingly changed topology of the Fermi surface will influence the exchange integrals between Mn spins despite the fact that the Mn sublattice is structurally perfect. Another consequence of a varying carrier concentration is the modification of the energy separation between the Fermi energy and the unoccupied Mn $3d$ states, which gives rise to an increased superexchange interaction and thus influences the values of the exchange integrals as follows from the Anderson s-d-mixing model.[9] This fact has recently been used in the context of Heusler alloys with

chemical disorder on the *sp* sublattice[10] and very recently also in related study of 3*d*-electron-induced magnetic phase transition in (Cu,Ni)MnSb and (Co,Ni)MnSb Heusler alloys.[5] Finally, the rather large Mn-Mn distance in Heusler alloys and the fact that four nearest neighbors (NNs) are empty sites give rise to relatively narrow Mn-spin subbands, so that the effect of electron correlations in the Mn subbands may be non-negligible.

It is the purpose of this paper to perform a computational simulation of the magnetic, thermodynamic, and transport properties of quaternary semi-Heusler (Cu,Ni)MnSb alloys in the framework of the density-functional formalism by including magnetic disorder for larger Cu concentrations. We have also investigated the robustness of the results with respect to the specific model of magnetic disorder on Mn sublattice used. The effect of electron correlations for Mn is included by means of a simple LDA+U (LDA, local-density approximation) approach.[11,12] The calculated results are finally compared in detail with available experimental data.

II. FORMALISM

The electronic structure calculations were performed using the tight-binding linear muffin-tin orbital (TBLMTO) approach. The effect of substitutional disorder on the Cu-Ni sublattice was described by the CPA.[13] The semi-Heusler alloys have a C_{1b} crystal structure which can be represented by four fcc-type sublattices (Cu,Ni)-Mn-*E*-Sb shifted along the [111] direction by $a/4$ each, where a is the lattice constant and the symbol E denotes the empty sublattice (interstitial sites). The same Wigner-Seitz radii for the constituent atoms were used in the calculations; the lattice constants obeying reasonably well Vegard's law were taken from experiment. For the parameterization of the local-density functional, the Vosko-Wilk-Nusair exchange-correlation potential[14] was used. The magnetic disorder was treated in the framework of the uncompensated disordered local-moment (DLM) (uDLM) model. In this model we assume the onset of magnetic disorder at some Cu concentration ($x_{\mathrm{Cu}} \approx 0.7$). The magnetic disorder is characterized by some amount x^{-}_{Mn} of Mn spins (with the local moment $m^{\mathrm{Mn}-}$) chosen randomly in the direction opposite to the rest of the x^{+}_{Mn} Mn spins (with the local moment $m^{\mathrm{Mn}+}$) in the reference FM state. Clearly, $x^{+}_{\mathrm{Mn}}+x^{-}_{\mathrm{Mn}}=1$ on the Mn sublattice. In the DLM state, which can be considered as a "dynamical" AFM state, we have $x^{+}_{\mathrm{Mn}}=x^{-}_{\mathrm{Mn}}=0.5$. One can imagine many possible scenarios for magnetic disorder. We have used the simplest one, namely, a linear increase in x^{-}_{Mn} with the Cu concentration starting from $x_{\mathrm{Cu}}=0.7$ and reaching the DLM state as $x_{\mathrm{Cu}}=1$ such that $x^{-}_{\mathrm{Mn}}=(5/3)(x_{\mathrm{Cu}}-0.7)$. It should be noted that the uDLM state can straightforwardly be described in terms of the CPA.[13] We have, however, tested also other simple models for the magnetic disorder (see Sec. III D).

The thermodynamic properties of the system can be described by a classical Heisenberg Hamiltonian, making use of a two-step model,[15,16]

$$H_{\mathrm{eff}} = -\sum_{i,j} J_{ij} \mathbf{e}_i \cdot \mathbf{e}_j, \tag{1}$$

where i,j are site indices, $\mathbf{e}_i$ is the unit vector pointing along the direction of the local magnetic moment at site i, and J_{ij} is the exchange integral between sites i and j. The exchange integrals, by construction, contain the atom magnetic moments, their positive (negative) values being indicative of FM (AFM) coupling. It should be noted that, for an evaluation of the exchange integrals, we assume a FM reference state. Because of small induced moments, in particular on the Cu-Ni sublattice, also $J^{\mathrm{Mn},Q}$ exchange integrals (Q=Cu,Ni) could in principle be considered. A proper inclusion of exchange integrals due to induced moments into the evaluation of the Curie temperature, however, is a delicate not yet completely understood problem. In a recent study[17] it was demonstrated that an optimal result for NiMnSb semi-Heusler alloys is obtained if one keeps in Eq. (1) only the exchange integrals between Mn spins. This approximation is further supported by the fact that only the first NNs $J^{\mathrm{Mn,Q}}$ (Q=Cu,Ni) contribute non-negligibly and that they have a small coordination number of 4 only (see also Ref. 4). Therefore, we limited ourselves to $J^{\mathrm{Mn,Mn}}$ exchange integrals for the whole concentration range of the (Cu,Ni)MnSb alloy.

As concerns the statistical part, we determine the Curie temperature corresponding to the effective Heisenberg model in Eq. (1) by making use of the mean-field (MFA) and the random-phase (RPA) approximations. The RPA-Curie temperatures are close to those obtained from Monte Carlo simulations.[4] The MFA estimate of the Curie temperature is defined by

$$k_B T_c^{\mathrm{MFA}} = \frac{2}{3} \sum_{i \neq 0} J_{0i}^{\mathrm{Mn,Mn}}, \tag{2}$$

where the sum extends over many NN shells. An improved description of finite-temperature magnetism is provided by the RPA, namely,

$$(k_B T_c^{\mathrm{RPA}})^{-1} = \frac{3}{2} \frac{1}{N} \sum_{\mathbf{q}} [J^{\mathrm{Mn,Mn}}(0) - J^{\mathrm{Mn,Mn}}(\mathbf{q})]^{-1}. \tag{3}$$

Here N denotes the order of the translational group applied and $J^{\mathrm{Mn,Mn}}(\mathbf{q})$ is the lattice Fourier transform of the real-space exchange integrals $J_{ij}^{\mathrm{Mn,Mn}}$. It can be shown that T_c^{RPA} is always smaller than T_c^{MFA}.[18] We have used up to 62 shells in the evaluation of Eq. (2) and for the lattice Fourier transform of $J^{\mathrm{Mn,Mn}}(\mathbf{q})$ in Eq. (3) after having tested the convergence with respect to the number of shells included. The estimated computational error corresponding to the chosen number of shells used in these calculations is below ± 5 K. For further details we refer the reader to Refs. 4, 16, and 18.

Without external magnetic field, there are essentially three different contributions to the resistivity of magnetic alloys: (i) phonon scattering; (ii) magnetic scattering due to thermodynamic fluctuations, which are largest at the Curie temperature and essentially determined by the spin-spin-correlation function;[19] and (iii) the residual resistivity due to the presence of chemical disorder on the Cu-Ni sublattice and also due to magnetic disorder on the Mn sublattice (for $x_{\mathrm{Cu}} > 0.7$).

The residual resistivity clearly dominates in the low-temperature regime and in this paper we will limit ourselves to this case. We determine the resistivity using the linear-response theory as formulated in the framework of the

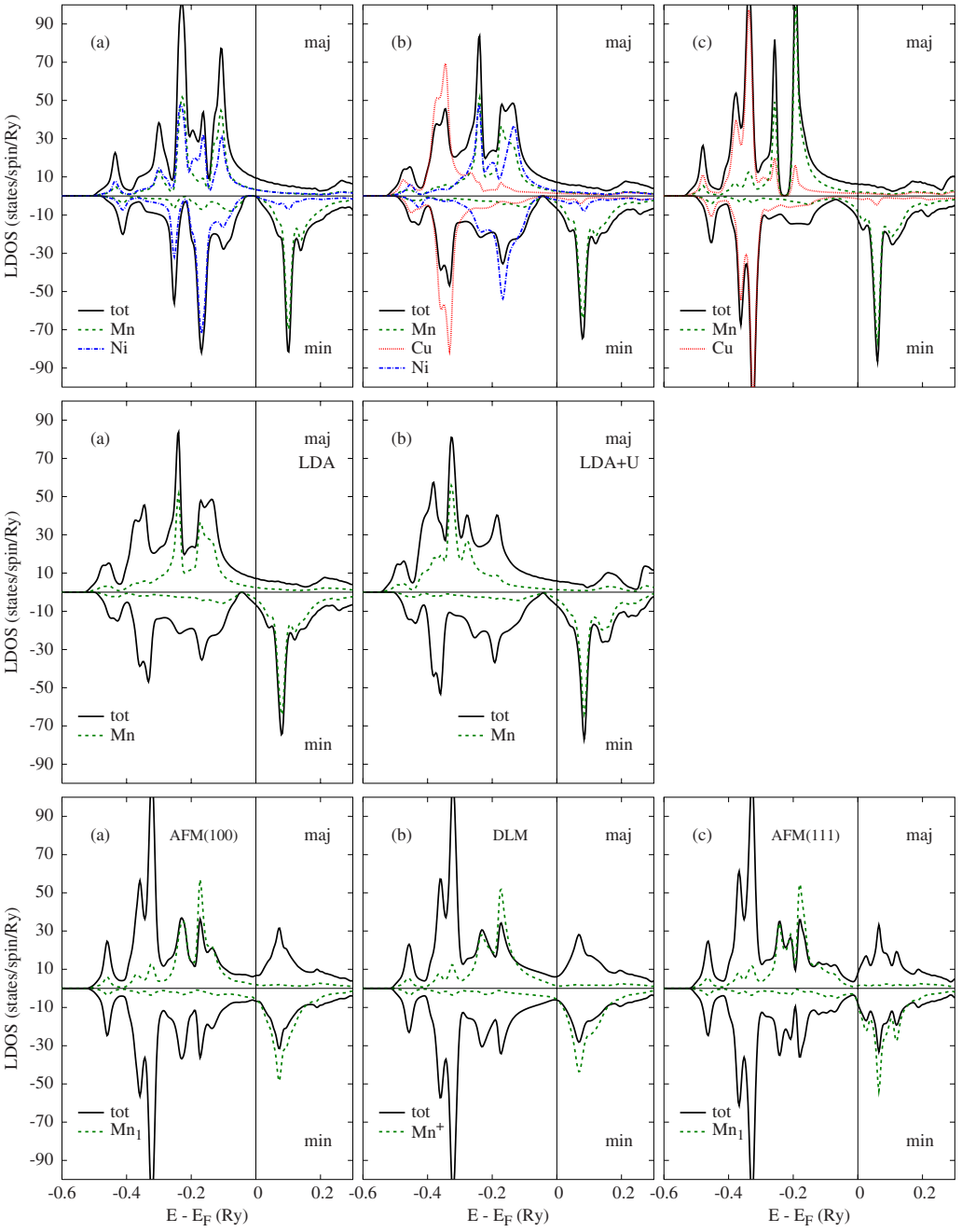

FIG. 1. (Color online) Total and component-resolved densities of states for FM (Cu,Ni)MnSb alloys. Top panel: (a) ordered NiMnSb, (b) disordered $(Cu_{0.5}Ni_{0.5})$MnSb, and (c) ordered CuMnSb. Middle panel: Total and Mn-resolved densities of states for disordered FM $(Cu_{0.5}Ni_{0.5})$MnSb. (a) LDA and (b) LDA+U. Bottom panel: Total and Mn-resolved densities of states for AFM CuMnSb. (a) AFM(100) layers in the fcc Mn sublattice, (b) the DLM state, and (c) AFM(111) layers in the fcc Mn sublattice. Local Mn moments are shown only for one of the equivalent Mn sublattices (Mn_1) or for one of the possible spin directions (Mn^+).

TBLMTO-CPA approach (Kubo-Greenwood formula),[20] i.e., on the same formal footing as the determination of exchange integrals and magnetic moments. The applied approach as formulated for the multisublattice case allows us to include both the substitutional disorder on the Cu-Ni sublattice as well as the magnetic disorder on the Mn sublattice on equal footing.[21] We have also implemented disorder-induced vertex corrections into the formalism.[22]

III. RESULTS AND DISCUSSION

In this section we present the results for electronic, magnetic, thermodynamic, and transport properties of (Cu,Ni)MnSb alloys over a broad range of concentrations. The results for LDA and LDA+U will be presented in parallel.

A. Electronic and magnetic properties

In the top panel of Fig. 1 the calculated densities of states

(DOSs) of NiMnSb, $(Cu_{0.5}Ni_{0.5})MnSb$, and CuMnSb in the FM state are shown. NiMnSb is a halfmetal (the Fermi energy lies in the gap of the minority states) while with increasing Cu content the alloy becomes metallic. Two important trends have to be mentioned: (i) The Fermi energy moves toward the unoccupied Mn states with increasing Cu content. This effect raises the superexchange part of exchange integrals and leads to strong modifications with respect to alloying (see Sec. III B and Refs. 9 and 10). (ii) The different positions of the Cu- and the Ni-local DOS indicate strong substitutional disorder in the energy region of (−0.4,−0.15) Ry below the Fermi energy [see Fig. 1(b)]. It should be noted that Mn-majority states hybridize strongly with Ni states [see Fig. 1(b)], whereas their hybridization with Cu states is weak. The minority Mn states only weakly hybridize with both Cu and Ni states due to their separation in energy.

The effect of electron correlations in the narrow Mn subbands is illustrated in the middle panel of Fig. 1 for the $(Cu_{0.5}Ni_{0.5})MnSb$ alloy. Electron correlations are treated in the LDA+U approximation assuming an effective Hubbard parameter $U_{\mathrm{eff}}=0.13$ Ry. This value (kept the same in all calculations) is smaller than that used, e.g., in (Ga,Mn)As (Ref. 11) but close to that used in related Heusler alloys.[12] The smaller value of U_{eff} is due to a better screening corresponding to a higher concentration of mobile carriers in Heusler alloys as compared to diluted magnetic semiconductors. As a result of electron correlations, the occupied majority Mn states are shifted to higher binding energies.

Finally, in the bottom panel of Fig. 1 we show the results for the total and the Mn-local DOSs for three possible realizations of an AFM state, namely, for layers of oppositely oriented spins along the [100] or [111] directions in the fcc Mn sublattice [AFM(100) and AFM(111), respectively] and for the DLM state. The experiment seems to indicate that the ground state is the AFM(111) one.[23] As can be seen, the DOSs of the occupied states are very similar in all cases. This indicates also a close similarity of the band energy parts of the total energy used in the mapping to the Heisenberg Hamiltonian and hence a weak dependence of the estimated exchange integrals on the reference state (see Sec. II).

The most detailed characterization of the disordered state is provided by Bloch spectral functions, the analogs of energy bands in ordered systems.[13] This fact is illustrated in Fig. 2 for $(Cu_{0.5}Ni_{0.5})MnSb$. The majority s,p bands above the Fermi energy are only weakly influenced by the Cu-Ni disorder and therefore closely resemble the corresponding energy bands of the host NiMnSb crystal (bottom and top panels, respectively). The minority states above the Fermi energy are dominated by Mn d states and, via hybridization, are influenced by the Cu-Ni disorder—the effect, however, is not strong. On the contrary, in the energy region of (−0.4,−0.15) Ry below the Fermi level, we observe strongly broadened states making it difficult to identify individual bands, i.e., we observe a situation typical for strong chemical disorder. It should be noted that the states at the Fermi energy, which are relevant for the residual resistivity, are only weakly influenced by disorder. The different positions of majority- and minority-spin bands (see Fig. 1) clearly indicate the presence of strong chemical disorder in the concentration regime where magnetic disorder is present ($x_{\mathrm{Cu}}>0.7$).

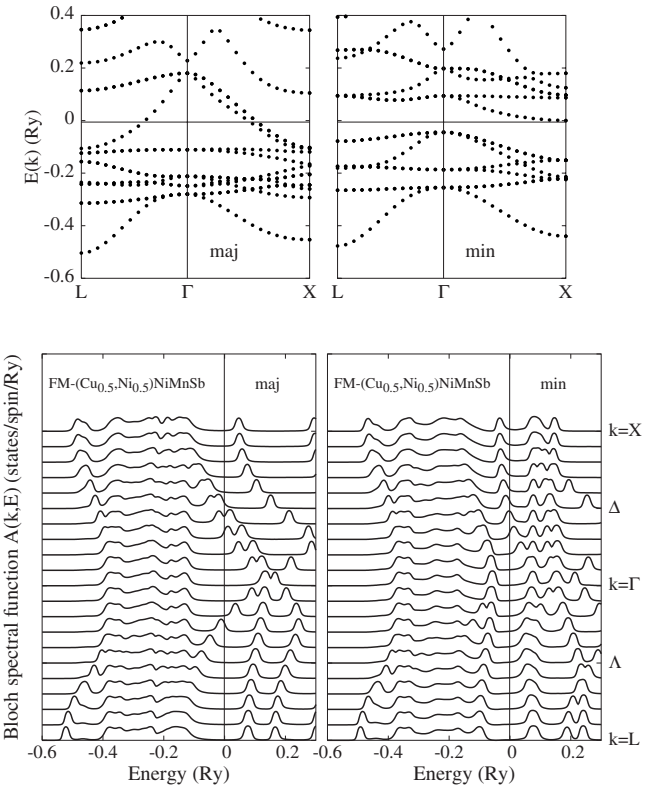

FIG. 2. Upper panel: Spin-resolved band structure of NiMnSb. Bottom panel: Bloch spectral functions for disordered FM $(Cu_{0.5}Ni_{0.5})MnSb$ along lines of high symmetry in the Brillouin zone as compared to the corresponding dispersion laws of the host NiMnSb alloy. Left (right) panels correspond to majority (minority) states.

In Fig. 3 we compare the concentration dependence of the calculated magnetic moments with available experiments.[7,8] We observe an overall very good agreement for the uDLM model over the whole concentration range for both the LDA and LDA+U models. It should be noted that calculations assuming an FM state, also for $x_{\mathrm{Cu}}>0.7$, fail to reproduce the experimental data. This fact is illustrated in Fig. 3(a) by empty circles (see also Ref. 5). The concentration dependence of local magnetic moments on Mn and Ni sites is generally weak. In particular, both Mn^{+} and Mn^{-} have almost the same sizes as expected for large robust magnetic moments. The induced moments on the Ni sublattice are rather small ($m^{\mathrm{Ni}}<0.5\ \mu_B$). We can thus conclude that a simple model of magnetic disorder is able to reproduce the experimental data quite well.

B. Exchange interactions and Curie temperatures

The concentration dependence of the exchange integrals is summarized in Fig. 4. The dominating exchange interactions $J_s^{\mathrm{Mn,Mn}}$ (s refers to the shell number) are shown in Fig. 4(a). The most remarkable feature is the reduction in the first NN coupling with increasing Cu content. Such a reduction is due to the increasing superexchange part of the exchange interaction resulting from the shift of the Fermi energy toward the unoccupied minority Mn states as discussed in Sec.

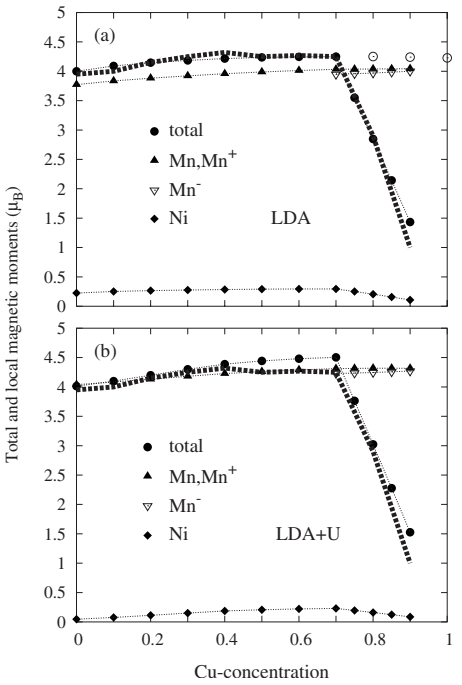

FIG. 3. Averaged and local magnetic moments as a function of composition for (Cu,Ni)MnSb alloys using an uDLM model. (a) LDA and (b) LDA+U. We also show the averaged moment for the ferromagnetic state, $x_{\mathrm{Cu}}>0.7$ [see the open circles in (a)]. Thick dashed lines denote the experimental data.[7] Note that Mn^{-} moments have to be taken with the opposite sign.

II. The superexchange interaction is negative and exponentially damped with the distance between sites; it therefore influences primarily the first NN couplings. Other couplings are only weakly concentration dependent. As a result, for low Cu content the first NN couplings dominate, but for high Cu content the second NN couplings become dominant. Our results confirm interpretation given recently in a related paper on the (Cu,Ni)MnSb and (Cu,Co)MnSb alloys.[5]

The concentrational trend of the intersublattice exchange interactions $J_1^{Q,\mathrm{Mn}}$ (Q=Cu,Ni) is shown in Fig. 4(b). All other interactions of this type are negligible. The $J_1^{Q,\mathrm{Mn}}$ depend very weakly on the composition. While the $J_1^{\mathrm{Cu,Mn}}$ are rather small, the $J_1^{\mathrm{Ni,Mn}}$ are comparable to $J_s^{\mathrm{Mn,Mn}}$ ($s=1,2$). However, as shown in Refs. 4 and 17, their effect on the Curie temperature is small and will therefore be neglected (see also Sec. II). The spatial range of the exchange interactions is illustrated in Fig. 5, where we show dominating interactions $d^3 J_s^{\mathrm{Mn,Mn}}$ as a function of the distance d along the fcc [110] direction. It should be noted that we have multiplied the exchange interactions by the Ruderman-Kittel-Kasuya-Yosida factor d^3. This allows us to see more clearly a possible damping of the interactions with distance. Due to the gap in the minority states, the exchange interactions in NiMnSb are exponentially damped as explained in Ref. 4. For metallic CuMnSb, on the contrary, we observe a well-pronounced oscillatory behavior. The oscillatory behavior in random $(\mathrm{Cu}_{0.5}\mathrm{Ni}_{0.5})$MnSb is damped due to (Cu,Ni) disorder, which indirectly influences the $J_s^{\mathrm{Mn,Mn}}$ exchange coupling in a similar manner as in the related case of Ni_{2-x}MnSb Heusler alloys.[4]

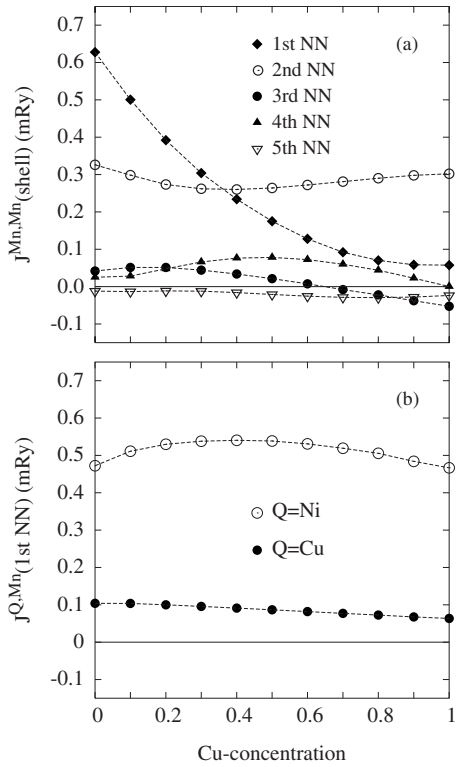

FIG. 4. Concentration dependence of exchange integrals in (Cu,Ni)MnSb Heusler alloys as estimated from the FM reference state. (a) the first five dominating (Mn,Mn) exchange integrals and (b) the dominating first NN (Mn,Q) exchange integrals (Q=Cu,Ni) between magnetic atoms on different sublattices.

The exchange integrals calculated in the framework of both the LDA and LDA+U approximations are then used to estimate the Curie temperatures [see Figs. 6(a) and 6(b), respectively]. Both the MFA and RPA estimates are shown and compared with the experiment. The smooth monotonic decrease in Curie temperatures with increasing Cu concentration as found in the experiment is reproduced by either approximations (MFA and RPA) and in both the LDA and

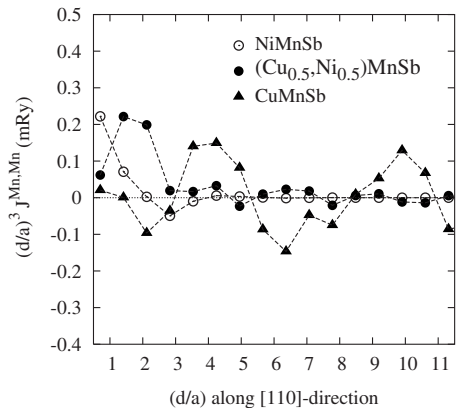

FIG. 5. (Mn,Mn) exchange integrals evaluated along the dominating [110] direction in the fcc sublattice for NiMnSb, disordered $(\mathrm{Cu}_{0.5}\mathrm{Ni}_{0.5})$MnSb, and CuMnSb Heusler alloys. The distance is measured in units of the lattice constant. Note that the exchange interactions are multiplied by $(d/a)^3$.

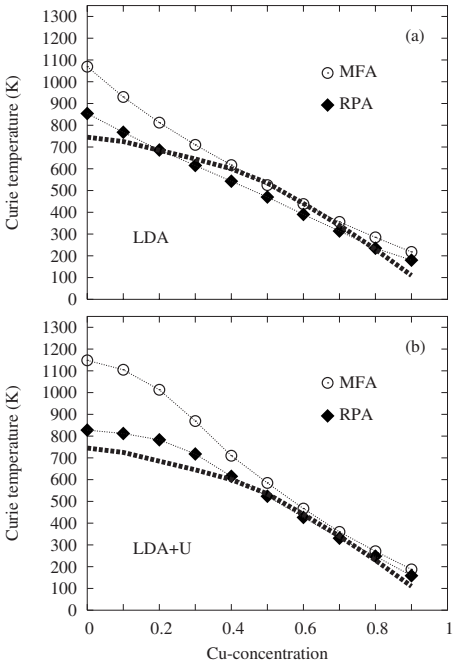

FIG. 6. Estimated Curie temperatures in the MFA and RPA. (a) LDA and (b) LDA+U. The thick dashed lines refer to the experimental data.[7]

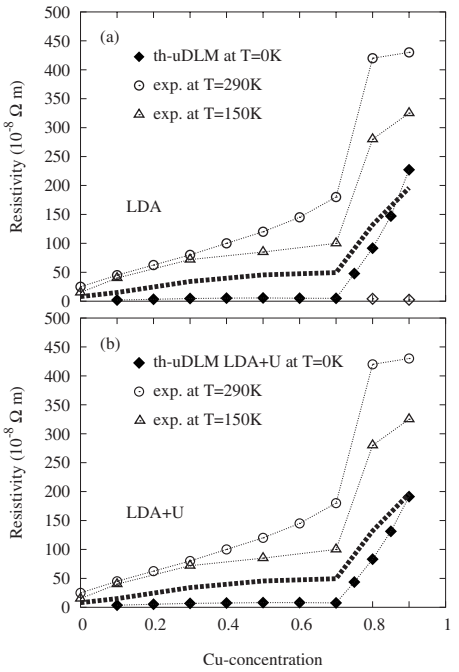

FIG. 7. Calculated residual resistivities. (a) LDA and (b) LDA+U. In both figures, the full diamonds denote the calculated resistivities (the uDLM model). The experimental values at $T=0$ K (thick dashed lines) were obtained by an extrapolation of the T-dependent resistivities.[7] For comparison also the resistivities for $T=290$ K and $T=150$ K are shown. In the case of the LDA, the results assuming the FM state for $x_{Cu}>0.7$ are also shown (empty diamonds).

LDA+U methods. The MFA overestimates Curie temperatures as to be expected, while an overall good agreement is found for the RPA. It seems that the LDA+U approach agrees better with the available experimental data, in particular, as the shape of the concentration dependence is concerned. The Curie temperature for NiMnSb and the LDA agrees with those obtained in Ref. 4.

C. Residual resistivities

The residual resistivities for the LDA and LDA+U models are shown in Fig. 7 together with the experimental results.[7] Since no experimental results for $T=0$ K were presented in Ref. 7, the values at $T=0$ K shown in this figure by thick dashed lines were obtained by a (linear) extrapolation of the measured temperature dependence of resistivities to $T=0$ K.[24] As can be seen in Fig. 7(a) the FM reference state (empty diamonds) fails to reproduce the experiment, even qualitatively, for $x_{Cu}>0.7$. On the contrary, the present uDLM model reproduces the resistivity (in particular, the sharp break at $x_{Cu}=0.7$) quite reasonably well for both the LDA and LDA+U approximations. It should be noted that the resistivities for $x_{Cu}<0.7$ are smaller than experimental ones extrapolated to $T=0$ K. This fact can have different origins, e.g., an error in the extrapolation of the measured resistivities to $T=0$ K or the presence of an additional resistivity due to possible native defects (interstitials, vacancies, swapping defects, etc.)[25] not considered in the present study.

D. Another scenario for the FM to AFM transition

We have already mentioned that there are many possible scenarios to describe the transition from the FM state to the AFM state. In the following we wish to investigate the robustness of our results by simply using the opposite case, namely, by starting from possible AFM states, namely, AFM(100) or AFM(111), sometimes called the AF I and AF II states (see e.g., Ref. 26). The transition from the AFM to the FM state is then realized by gradually converting the orientations of spins (on the sublattice with oppositely oriented moments) such that at the end we obtain the FM state (in a doubled cell). In this particular approach it is found that concentration dependence of the averaged magnetic moments is almost identical to that one shown in Fig. 3. This is easy to understand by invoking the results shown in the bottom panel of Fig. 1. The residual resistivity, on the contrary, is very sensitive to details of scattering on defects and it is thus a crucial test of the dependence of results of the FM to an AFM transition scenario. The results for the resistivity of the AFM(100) and AFM(111) models are compared with the previously used uDLM model (see Fig. 7) and presented in Figs. 8(a) and 8(b) for the LDA and LDA+U, respectively. The smaller resistivity of the AFM(100) model as compared to the AFM(111) model is due to the smaller spatial distances between disordered [111] planes with oppositely oriented layers as compared to the [100] planes. However, despite some differences in the resistivities, one can conclude that the results discussed in this paper are consistent with respect to the choice of details of the scenario for the FM to AFM transition.

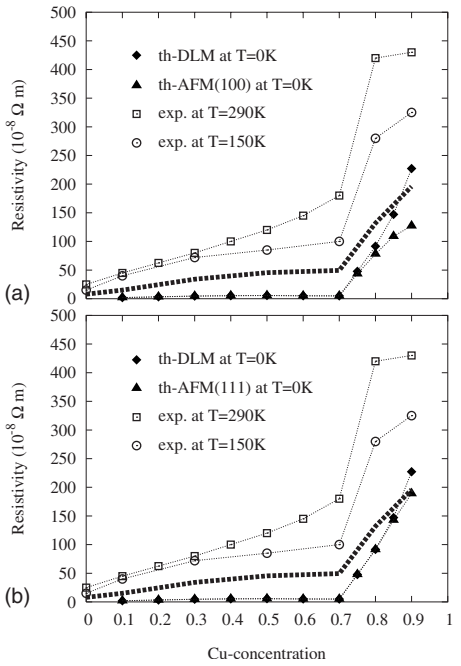

FIG. 8. Calculated residual resistivities for various scenarios of the transition between the FM and AFM states using LDA for (a) the AFM(100) reference state (top) and (b) the AFM(111) reference state (bottom). The various entries are listed explicitly within the figure. The experimental values at $T=0$ K (thick dashed lines) were obtained by an extrapolation of the T-dependent resistivities.[7] For comparison also the resistivities for the uDLM model (see also Fig. 7) are shown.

E. Electronic origin of the FM to AFM transition

The final question we wish to address is the origin of the break in the concentration dependence of the magnetization and the resistivity for $x_{\mathrm{Cu}} \in (0.7, 0.8)$ by investigating the stability of the FM state with respect to periodic spin-density fluctuations. The underlying idea is the same as that one used to study the stability of the disordered phase with respect to periodic charge-density fluctuations (effective Ising model[27]). This approach allows us to estimate possible ordered phases, which can form from a disordered phase on a given lattice. We shall therefore employ the same approach, however, applied here to the classical Heisenberg model in Eq. (1) by determining possible magnetic phases on a given lattice. For this purpose we calculated the lattice Fourier transform $J^{\mathrm{Mn,Mn}}(\mathbf{q})$ of the real-space exchange integrals $J_s^{\mathrm{Mn,Mn}}$ and searched for its maximum which, due to the sign convention in Eq. (1), corresponds to the ground state (the energy minimum). The concentration dependence of $J^{\mathrm{Mn,Mn}}(\mathbf{q})$ as evaluated for the FM reference states is shown in Fig. 9. We clearly observe a pronounced maximum at $\mathbf{q}=0$ for NiMnSb. This means that the energy is minimized by spin fluctuations with an infinitely large wavelength implying in turn that the FM ground state is formed. With increasing Cu concentration, the stability of the FM state decreases until $x_{\mathrm{Cu}} \approx 0.8$ at which concentration the FM state decays into a more complex magnetic state and finally, for $x_{\mathrm{Cu}}=1$, the AFM state is formed. It is very tempting to identify this transition with the onset of the magnetic disorder on the Mn sublattice. For $x_{\mathrm{Cu}}=1$ or CuMnSb we found the minimum at $\mathbf{q}=X$, which corresponds to the AFM(100) state rather than to the experimentally observed AFM(111) state.[23]

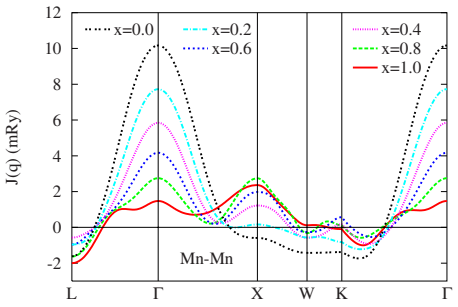

FIG. 9. (Color online) Lattice Fourier transform of (Mn,Mn) exchange interactions for various Cu concentrations x of (Cu,Ni) MnSb alloys. $x=0$ and $x=1$ thus corresponds to NiMnSb and CuMnSb alloys, respectively. Because of sign convention in Eq. (1), for a given alloy composition, the maximum indicates the minimum of energy or the ground state.

The magnetic phase diagram of the Ising model (i.e., the Heisenberg model with collinear spins) for two NN couplings J_1 and J_2 is well known.[27] The AFM(100) phase is stabilized if J_2 is FM coupling and J_1 is AFM coupling. The calculated J_2 is FM, but J_1 is also FM although very small (see Fig. 4). We have verified that in accordance with the above model, $J^{\mathrm{Mn,Mn}}(\mathbf{q})$ for two NN couplings has a weak maximum at $\mathbf{q}=0$. The well-pronounced maximum at $\mathbf{q}=X$ is only obtained using a large enough set of calculated exchange interactions (see Fig. 9). The stability region of the AFM(111) phase seems to be more complex; however, the necessary condition for its occurrence is that the J_2 is AFM. We have checked that a lattice-constant variation of $\pm 5\%$ will not change the sign of the calculated J_2. We also calculated total energies for both the AFM(100) and AFM(111) phases leading to the same conclusion, namely, that the AFM(100) has the lowest energy. In Ref. 6 only the total energies of the AFM(111) and FM phases are compared with each other but not with the AFM(100) phase.

It should be noted that, for AFM CuMnSb, the contradicting experimental results obscure a final assessment of the type of ordering present: while low-temperature resistivity studies indicate pronounced defect disorder, in structural investigations, such a disorder was not traced.[28] It seems therefore that more experimental and theoretical studies are needed to sort out this obvious discrepancy.

IV. CONCLUSIONS

We have studied the electronic, magnetic, thermodynamic, and transport properties of quaternary semi-Heusler alloys (Cu,Ni)MnSb theoretically by means of an *ab initio* approach based on the density functional. A simple model of magnetic disorder on the Mn sublattice with the onset at approximately 70% of Cu successfully explains available experimental data. In particular, the break in the magnetization and the resistivity is found to occur at the experimentally

detected concentration. The monotonic decrease in the Curie temperature with increasing Cu concentration is also reproduced properly. The RPA method provides a satisfactorily quantitative agreement between theory and experiment (the error being less than 10%–15%). We also demonstrated that results shown are independent of the specific model of magnetic disorder used in the numerical modeling. Finally, we showed that the FM phase decays into a complex magnetic state at about 80% of Cu, which can be considered as an indication of the onset of the magnetic disorder.

ACKNOWLEDGMENTS

This study was carried out within the project AVOZ (Project No. 10100520) of the Academy of Sciences of the Czech Republic. J.K. and V.D. acknowledge the financial support from the Grant Agency of the Academy of Sciences of the Czech Republic (Grant No. A100100616), the Czech Science Foundation (Grant No. 202/07/0456), and COST P19 (Grant No. OC150). The work of I.T. is part of research program MSM (Project No. 0021620834) financed by the Ministry of Education of the Czech Republic.

[1] I. Galanakis, P. H. Dederichs, and N. Papanikolaou, Phys. Rev. B **66**, 174429 (2002).
[2] E. Sasioglu, L. M. Sandratskii, and P. Bruno, Phys. Rev. B **70**, 024427 (2004).
[3] P. J. Webster and K. R. A. Ziebeck, in *Alloys and Compounds of d-Elements with Main Group Elements*, Landolt-Börnstein, New Series, Group III, Vol. 19c, Pt. 2, edited by H. R. J. Wijn (Springer, Berlin, 1988).
[4] J. Rusz, L. Bergqvist, J. Kudrnovský, and I. Turek, Phys. Rev. B **73**, 214412 (2006).
[5] I. Galanakis, E. Sasioglu, and K. Ozdogan, Phys. Rev. B **77**, 214417 (2008).
[6] T. Jeong, R. Weht, and W. E. Pickett, Phys. Rev. B **71**, 184103 (2005).
[7] S. K. Ren, Y. X. Wang, Y. J. Zhang, G. B. Ji, F. M. Zhang, and Y. W. Du, J. Alloys Compd. **387**, 32 (2005).
[8] S. K. Ren, W. Q. Zou, J. Gao, X. L. Liang, F. M. Zhang, and Y. W. Du, J. Magn. Magn. Mater. **288**, 276 (2005).
[9] P. W. Anderson, Phys. Rev. **124**, 41 (1961).
[10] E. Sasioglu, L. M. Sandratskii, and P. Bruno, Appl. Phys. Lett. **89**, 222058 (2006).
[11] A. B. Shick, J. Kudrnovský, and V. Drchal, Phys. Rev. B **69**, 125207 (2004).
[12] B. Balke, G. H. Fecher, H. C. Kandpal, C. Felser, K. Kobayashi, E. Ikenaga, J.-J. Kim, and S. Ueda, Phys. Rev. B **74**, 104405 (2006).
[13] I. Turek, V. Drchal, J. Kudrnovský, M. Šob, and P. Weinberger, *Electronic Structure of Disordered Alloys, Surfaces and Interfaces* (Kluwer, Boston, 1997); I. Turek, J. Kudrnovský, and V. Drchal, in *Electronic Structure and Physical Properties of Solids*, Lecture Notes in Physics Vol. 535, edited by H. Dreyssé (Springer, Berlin, 2000), p. 349.
[14] S. H. Vosko, L. Wilk, and M. Nusair, Can. J. Phys. **58**, 1200 (1980).
[15] A. I. Liechtenstein, M. I. Katsnelson, V. P. Antropov, and V. A. Gubanov, J. Magn. Magn. Mater. **67**, 65 (1987).
[16] I. Turek, J. Kudrnovský, V. Drchal, and P. Bruno, Philos. Mag. **86**, 1713 (2006).
[17] L. M. Sandratskii, R. Singer, and E. Sasioglu, Phys. Rev. B **76**, 184406 (2007).
[18] M. Pajda, J. Kudrnovský, I. Turek, V. Drchal, and P. Bruno, Phys. Rev. B **64**, 174402 (2001).
[19] M. E. Fisher and J. S. Langer, Phys. Rev. Lett. **20**, 665 (1968).
[20] I. Turek, J. Kudrnovský, V. Drchal, L. Szunyogh, and P. Weinberger, Phys. Rev. B **65**, 125101 (2002).
[21] I. Turek, J. Kudrnovský, V. Drchal, and P. Weinberger, J. Phys.: Condens. Matter **16**, S5607 (2004).
[22] K. Carva, I. Turek, J. Kudrnovský, and O. Bengone, Phys. Rev. B **73**, 144421 (2006).
[23] K. Endo, T. Okoyama, and R. Kimura, J. Phys. Soc. Jpn. **25**, 907 (1968).
[24] The concentration dependence of resistivities is presented in Ref. 7 only for $T=290$ K but presented data allows to extract also results for $T=150$ K. Results for $T=0$ K were obtained by a linear extrapolation of measured results. While some error is probably introduced, we believe that the trend is reproduced correctly.
[25] B. Alling, S. Shallcross, and I. A. Abrikosov, Phys. Rev. B **73**, 064418 (2006).
[26] J. Kübler, A. R. Williams, and C. B. Sommers, Phys. Rev. B **28**, 1745 (1983).
[27] F. Ducastelle, *Order and Phase Stability in Alloys* (North-Holland, Amsterdam, 1993).
[28] J. Boeuf, C. Pfleiderer, and A. Faiszt, Phys. Rev. B **74**, 024428 (2006).